Modeling Ire1p Regulation and Activation in the Yeast UPR

Scott Hildebrandt[*], David Raden[†], Anne Skaja Robinson[†], and Francis J. Doyle III[*1]

[*]Department of Chemical Engineering

University of California, Santa Barbara

Santa Barbara, CA 93106

[†]Department of Chemical Engineering

University of Delaware

Newark, DE 19716

Key words: Unfolded Protein Response, *Saccharomyces cerevisiae*, Ire1p

mathematical modeling, sensitivity analysis

November 2006

Unpublished

[1]Author to whom correspondence should be addressed: frank.doyle@icb.ucsb.edu

Modeling Ire1p Regulation and Activation in the Yeast UPR

Scott Hildebrandt*, David Raden†, Anne Skaja Robinson†, Francis J. Doyle III*
*University of California Santa Barbara, Santa Barbara, CA, U.S.A
†University of Delaware, Newark, DE, U.S.A.

Introduction

Saccharomyces cervisiae, or bakers' yeast, are utilized in the biotechnology industry to express, fold, and assemble foreign protein therapeutics [1]. Simply modifying yeast to express high levels of heterologous protein does not necessarily maximize production and secretion, as this action triggers the Unfolded Protein Response (UPR), which eliminates quantities of desired protein through promoted ER-Associated Degradation (ERAD). The yeast UPR may even retard transcription and/or translation of the desired protein, thus decreasing yields. Consequently, a combined approach of mathematical modeling and experiments has been employed in an attempt to obtain a thorough understanding of the yeast UPR, which will be utilized to forward engineer the system to maximize foreign protein therapeutic production.

The yeast UPR has been traditionally modeled as the negative feedback loop shown in Figure 1 in which low levels of the chaperone BiP (Binding Protein) relative to unfolded protein (UP) in the ER signal the need for increased production of UPR component proteins--including BiP--that help cells cope with these high ER UP levels. The UPR signal is transduced from the ER to the nucleus and cytoplasm by the ER membrane-spanning endonuclease Ire1p, which enhances translation of Hac1p, a transcription factor that upregulates BiP and other UPR-related gene expression. Traditional modeling identifies BiP as the primary regulator of Ire1p: BiP typically binds Ire1p but is sequestered exclusively by UP when UP is in excess; unbound Ire1p is then free to dimerize, *trans*-autophosphorylate, and transduce the UPR signal across the nuclear ER membrane [2,3]. However, recent experimental evidence suggests BiP may simply serve as an adjustor or modulator in Ire1p activation and that UP directly regulates Ire1p activation instead [4,5].

This work sought to identify and define fundamental differences, using mathematical modeling and systems analysis tools, between the traditional and newer Ire1p activation models where BiP serves as the primary activation regulator, UP does alone, and UP does combined with modulation by BiP. These three activation models are the BiP-Ire1p (BI), UP-Ire1p (UPI), and BiP-modulated (BM) models, respectively, represented schematically in Figure 2. Once the fundamental differences had been identified, they served as a foundation upon which experimental protocols could be designed to determine which model best characterizes the biological behavior.

Materials and Methods

A mechanistic, deterministic mathematical model of the yeast UPR was developed and implemented in the Matlab Simulink environment using the ode15s solver. This model contained 32 states that described the interactions between the major UPR components--UP,
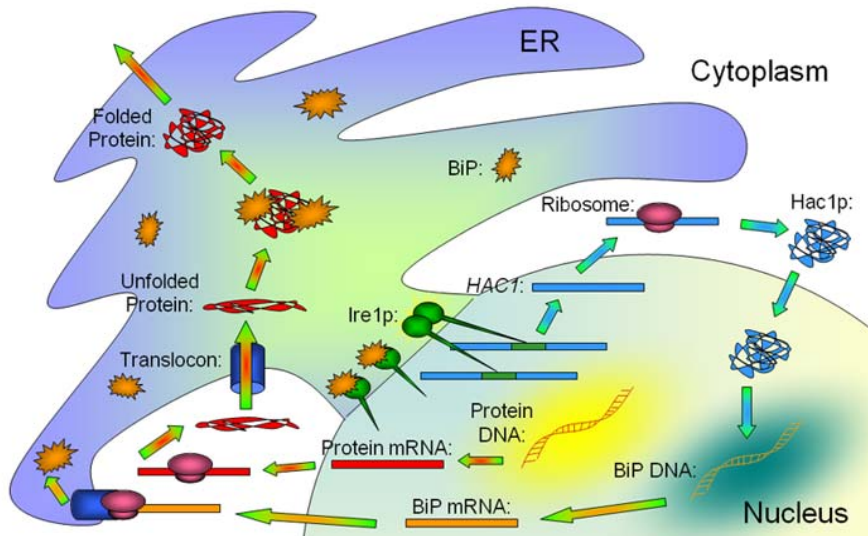
Figure 2. UPR schematic based on traditional Ire1p regulation model that includes all steps captured in the mathematical models. Unfolded protein enters the ER and draws BiP away from Ire1p. Unbound Ire1p is free to dimerize and *trans*-autophosphorylate. Active Ire1p splices an intron from *HAC1*, and only then can it be translated. Hac1p binds the UPRE promoter sequence in front of the KAR2 gene, and BiP transcription is upregulated. Thus, the UPR is induced.
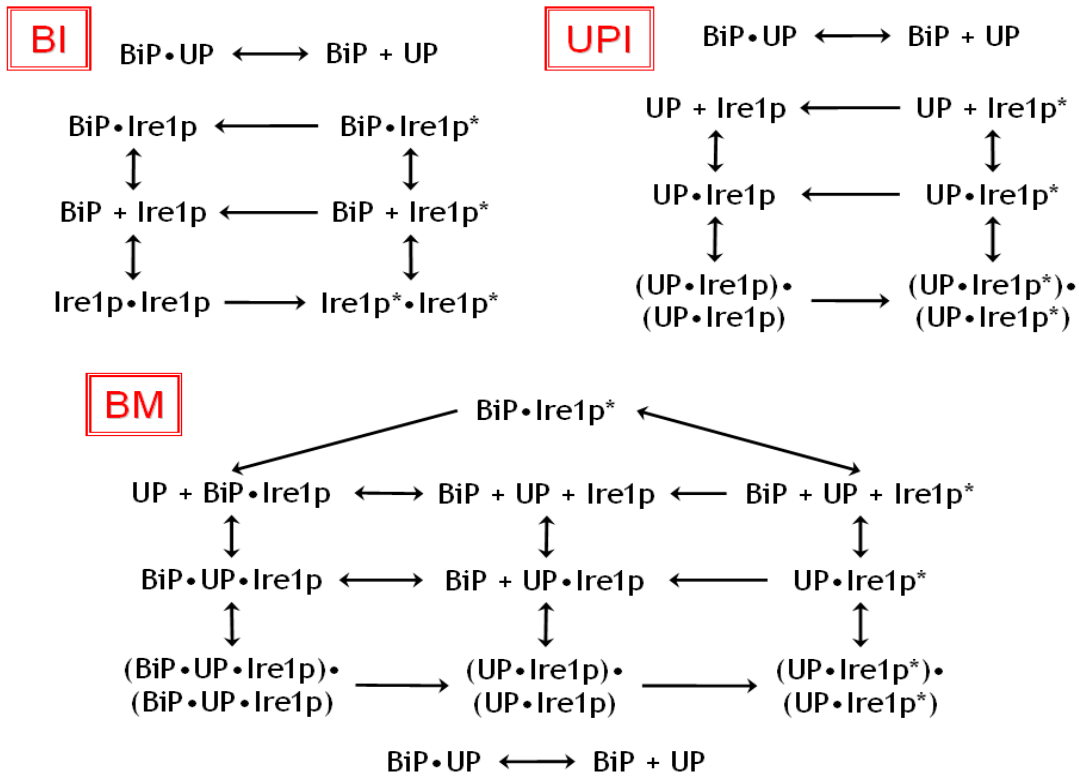

Figure 1. Schematics for the BI, UPI, and BM Ire1p regulation models. In the BI model, Ire1p activation takes place in the absence of BiP binding; in the UPI model, it activates only in the presence of UP binding; and in the BM model, it activates only when both of these events occur. Activated Ire1p is represented as "Ire1p*."

Hac1p, and BiP--as well as two critical UPR inducers--heterologous scFv and DTT. The three Ire1p activation models were then substituted into this general UPR model framework.

At first, parameter values for the models' mass-action kinetic ODEs were largely taken from the literature, based upon experimental data from systems of varying applicability to the one at hand (i.e., *in vitro* ones, ones in other organisms, and/or ones with homologous species). However, this literature-based parameter set did not give all desired protein levels and other model characteristics, so some were tuned using parameter optimization routines like Matlab's FMINCON and/or an evolutionary algorithm. A summary of the desired model characteristics and the parameters that were adjusted to fit the data is provided in Table 1.

Table 1. List of model characteristics and the parameters that were optimized in order to fit the available data. These characteristics were in the uninduced and 5 mM DTT- and scFv-induced UPR states.

Uninduced

Desired	Actual	Fit Parameters
3.37e5 BiP	3.37e5 BiP	BiP transcription, UP-ER entry
1.5e5 UP	1.5e5 UP	BiP transcription, UP-ER entry
2.53e7 ER residents (excluding BiP)	2.53e7 ER residents (excluding BiP)	protein turnover
1 Ire1p*	1.15 Ire1p*	BiP- or UP-Ire1p binding and dissociation
low HAC1 splicing	1.32% HAC1 splicing	none directly
low Hac1p	189 Hac1p	none directly
low KAR2 UPRE binding	7.81% KAR2 UPRE binding	none directly

5 mM DTT-Induced

Desired	Actual	Fit Parameters
1.5e7 UP	1.5e7 UP	disulfide-bonded protein denaturation by DTT
258 Ire1p*	233 Ire1p*	BiP- or UP-Ire1p binding and dissociation
99% HAC1 splicing	75% HAC1 splicing	HAC1 transcription and splicing
8.97e3 Hac1p	8.97e3 Hac1p	HAC1 transcription and splicing
90% KAR2 UPRE binding by two Hac1p	88.5% KAR2 UPRE binding	UPRE binding and dissociation

scFv-Induced

Desired	Actual	Fit Parameters
GFP trajectory similar to experimental data	GFP trajectory similar to experimental data	scFv-ER entry, binding by BiP, chaperoned and unchaperoned folding, and degradation

When the Ire1p models' behavior was shown to be largely similar for traditional scFv (single chain antibody 4-4-20 expression)- and DTT-induced UPRs, sensitivity analysis was performed on the models using the BioSens software package for BioSpice, which runs .bsn versions of the models in DASPK, to probe for more obscure discrimination criteria. Sensitivity analysis measures changes in output (*x*) for a given change in parameter value (*p*), according to:

$$S_{ij} = \left(p_j \frac{\partial x_i}{\partial p_j} \right)_{x=x(t,p_0), p=p_0} \tag{1}$$

In Equation 1, the sensitivity has been parameter-scaled.

A GFP reporter was used to indicate UPR levels both experimentally and in the mathematical models. This state's mean parameter- and state (mean state values were used)-

scaled sensitivities were compared across the Ire1p models for runs performed under three different sets of conditions: 100-h uninduced, 5-h DTT-induced, and 10-h scFv-induced UPRs. Additionally, for each model, sensitivities were compared across the three condition sets.

Sensitivity comparison comprised of two calculations. First, the absolute difference between the sensitivities was taken, and it was decided values < 0.5 indicated sensitivities that were too similar when comparing across models, 0.1 when comparing across conditions. Second, the following calculation was performed:

$$\frac{|S_1 - S_2|}{\max\left(|S_1|, |S_2|\right)} \tag{2}$$

A value of 0.99 or more guaranteed same-sign sensitivities were at least two orders of magnitude apart.

Results

Parameter optimization on the Ire1p activation models yielded three models with largely similar steady-state and scFv- and DTT-induced UPR behavior. Figure 3 demonstrates this result for the scFv response, where there was only a small difference between BI and UPI/BM behaviors: UPR induction was slightly delayed, and recovery was somewhat hastened in the BI versus the UPI/BM models. This discrepancy likely stems from the contrast between indirect and direct Ire1p activation found in the respective models. That is, it takes longer for BiP to be drawn away from Ire1p in the BI model than it takes for unfolded scFv to bind Ire1p directly to activate it in the UPI/BM models (note that the irreversible BiP release step from the BiP•UP•Ire1p dimer, shown in Figure 2, makes the BM model behave more like the UPI than BI model in this and most respects). Conversely, it takes less time for the scFv to simply be bound by BiP (which is sufficient to begin shutting off the UPR in the BI model) than it takes for it to be bound and folded (necessary to begin shutting off the UPR in the UPI/BM models), so recovery occurs more quickly in the BI than UPI/BM models.
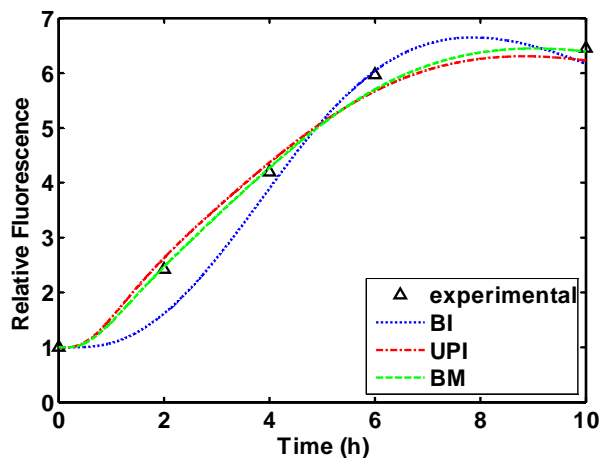

Figure 3. scFv-induced UPR responses for the models and experiment. Relative fluorescence units reflect relative GFP levels, which were used to report relative UPR induction. Model parameters (scFv entry to the ER, BiP binding to scFv, scFv degradation, and self- and chaperoned scFv folding rates) were fit to capture the experimental data and a heuristic value of $\sim5\times10^4$ scFvs at t=10 h. These scFv values were 2.0×10^5, 1.7×10^5, and 1.8×10^5 for the BI, UPI, and BM models, respectively. Experimental data from Raden, et al. [6].

With the three Ire1p models equally capable of reproducing experimentally-observed UPR behavior, a systems analysis tool was employed to search for other model discrimination criteria that could then be used to design experiments to distinguish the model most representative of the biological system. This tool, sensitivity analysis, comprehensively searches the models' structure for robust components and fragilities unique to fundamentally different models. It performs this task by evaluating the dependence of the models' outputs on their parameter values.

The sensitivities were compared across models for the uninduced and scFv- and DTT-induced UPR states. Again, results for the UPI and BM models were nearly identical. In the steady-state, UPI/BM sensitivities to BiP-general protein-binding and Ire1p* dimerization rates were significantly greater than those for the BI. In addition to this result being true in the scFv-induced UPR state, the UPI/BM models were significantly more sensitive to BiP-scFv binding than the BI model, and their sensitivities were of opposite signs.

When comparing across conditions, there was a set of parameter sensitivities that varied significantly between conditions for all Ire1p activation models: the scFv-induced UPR state was more sensitive to chaperoned protein folding and the amount of UP entering the ER than the DTT-induced state; and the undinduced state was more sensitive to BiP/GFP mRNA degradation, BiP degradation, and BiP cotranslational translocation than the DTT-induced UPR state. As for model-specific conditional parameter sensitivities, the UPI/BM models were significantly more sensitive to BiP-general UP binding in both the uninduced and the scFv-induced states than in the DTT-induced state, whereas the BI model was not. Additionally, the UPI/BM models were more sensitive to UP entry to the ER in the uninduced versus DTT-induced state, but the BI model was not.

Discussion

Two of these sensitivity analysis results stand out as strong candidates for model-invalidating experiment design. First, from the comparison across models in the scFv-induced UPR state, the widely-different, opposite-signed BiP-scFv binding rate sensitivities between the BI and UPI/BM models suggest an experiment that alters this rate could readily discriminate between the models. For example, this rate could be reduced by mutating BiP-binding sites on the scFv, and the effect on the UPR observed. If the rate reduction also reduced the UPR, the experiment would invalidate the UPI/BM models; if it increased it, it would invalidate the BI model (modeling results shown in Table 2). Performing these mutations would also likely decrease the scFv folding rate but the model discrimination would not be greatly altered, as shown in Table 2.

Second, from the comparison across conditions, no models were significantly sensitive to changes in UP entry to the ER in the DTT state, so the fact that the UPI/BM models were more sensitive to this parameter in the uninduced state and the BI model was not (all models are positively sensitive to this parameter) suggests another experimentally-testable distinction between the models. Upon decreasing/increasing UP-ER entry through a variety of experimental procedures, a stronger observed, respective decrease/increase in UPR would invalidate the BI model, and a weaker one would invalidate the UPI/BM models (Table 3). It should be noted

that, due to the subjective nature of labeling UPR decreases/increases "strong" or "weak," this second model discrimination experiment would best serve as a supplement to the first one with its well-defined model invalidation conditions.

Table 2. Effects on the scFv-induced UPR of reducing BiP-scFv binding, scFv folding, and both (bind-fold in Table) rates at once for the three Ire1p regulation models. Actual GFP molecule counts are provided as a measure of UPR induction. Reducing binding reduces the UPR in the BI model and increases it in the UPI/BM models. Reducing folding increases the UPR in all of the models. Combining the two effects gives behavior similar to reducing binding alone.

Model	UPR measure	nominal parameters	0.1×binding	0.001× binding	0.00001× binding	0.1×folding	0.001× folding	0.00001× folding	0.1×bind-fold	0.001× bind-fold	0.00001× bind-fold
BI	end GFP	905	883	372	150	1990	1990	1990	1989	1967	838
	mean GFP	641	627	288	149	1179	1210	1210	1176	1145	351
UPI	end GFP	914	1567	1989	1991	1732	1846	1847	1838	1992	1992
	mean GFP	661	1468	1826	1827	956	1001	1001	1568	1828	1829
BM	end GFP	949	1539	1965	1966	1669	1765	1766	1789	1966	1966
	mean GFP	669	1430	1803	1804	929	966	966	1516	1804	1804

Table 3. Effects of decreasing/increasing UP entry to the ER (V_{UP}) on the three Ire1p regulation models, starting from the uninduced UPR state. The UPI/BM models are more sensitive to changes in this parameter.

Model	UPR measure	nominal parameters	0.1×VUP	0.001×VUP	10×VUP	100×VUP	1000×VUP
BI	end GFP	147	147	147	147	147	1990
	mean GFP	147	141	141	258	1415	1984
UPI	end GFP	147	1	0	963	1919	1992
	mean GFP	147	1	1	1046	1967	1986
BM	end GFP	148	1	0	1034	1910	1973
	mean GFP	148	1	1	1114	1951	1967

One final issue regards further discrimination between the UPI and BM models, lest the BI model be invalidated. Other experiments do observe that BiP is bound to Ire1p in the uninduced UPR state and is not when the UPR is induced, regardless of the causal nature of the situation [4]. With this the case, the UPI model is invalidated as a wholly mechanistic representation of the biology. However, it has been shown that this model mimics the BM model in nearly every respect for uninduced and scFv- and DTT-induced UPRs and would be just as successful in capturing the associated biological behaviors. Since the less-complex UPI model is simpler to implement and manipulate computationally, it may be more amenable to certain *in silico* studies, so it should not be totally disregarded.

In conclusion, through the use of a powerful systems analysis tool, sensitivity analysis, mathematical modeling has presented experimental procedures to discriminate between competing hypothesized Ire1p regulation/activation models when none were readily apparent. While providing biological insight, these discrimination experiments will ensure future modeling studies properly capture and predict UPR behavior under a variety of conditions as they turn towards attempting to forward-engineer the system. A better-characterized system is also an asset to experimentalists as they endeavor to manipulate it.

References

[1] A. S. Robinson and D. A. Lauffenburger. Model for ER Chaperone Dynamics and Secretory Protein Interactions. *AIChE Journal*, 42(5): 1443-1453, 1996.

[2] A. A. Welihinda and R. J. Kaufman. The unfolded protein response pathway in *Saccharomyces cerevisiae.* Oligomerization and trans-phosphorylation of Ire1p (Ern1p) are required for kinase activation. *J. Biol. Chem.*, 271(30): 18181-18187, 1996.

[3] K. Okamura, Y. Kimata, H. Higashio, A. Tsuru, and K. Kohno. Dissociation of Kar2p/BiP from an ER sensory molecule, Ire1p, triggers the unfolded protein response in yeast. *Biochem. Biophys. Res. Commun.*, 279(2): 445-450, 2000.

[4] Y. Kimata, D. Oikawa, Y. Shimizu, Y. Ishiwata-Kimata, and K. Kohno. A role for BiP as an adjustor for the endoplasmic reticulum stress-sensing protein Ire1. *J. Biol. Chem.*, 167(3): 445-456, 2004.

[5] J. J. Credle, J. S. Finer-Moore, F. R. Papa, R. M. Stroud, and P. Walter. On the mechanism of sensing unfolded protein in the endoplasmic reticulum. *PNAS*, 102(52): 18773-18784, 2005.

[6] D. Raden, S. Hildebrandt, P. Xu, E. Bell, F. J. Doyle III, and A. S. Robinson. Analysis of cellular response to protein overexpression. *IEE Proc. Sys. Biol.*, 152(4): 285-289, 2005.